

## Full Length Article

## Towards carbon monoxide sensors based on europium doped cerium dioxide

P.P. Ortega<sup>a,\*</sup>, L.S.R. Rocha<sup>a</sup>, J.A. Cortés<sup>a</sup>, M.A. Ramirez<sup>a</sup>, C. Buono<sup>b</sup>, M.A. Ponce<sup>b</sup>, A.Z. Simões<sup>a</sup><sup>a</sup> São Paulo State University (UNESP) – School of Engineering of Guaratinguetá, Av. Dr. Ariberto Pereira da Cunha 333, Portal das Colinas, 12.516-410, Guaratinguetá, São Paulo, Brazil<sup>b</sup> University of Mar del Plata (UNMDP), Institute of Materials Science and Technology (INTEMA), National Research Council (CONICET), Av. Juan B. Justo 4302, 7600 Mar del Plata, Argentina

## ARTICLE INFO

## Keywords:

Cerium dioxide  
Thick films  
Gas sensor  
Carbon monoxide

## ABSTRACT

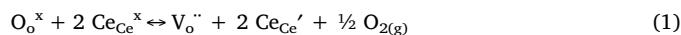
Ce<sub>1-(3/4)x</sub>Eu<sub>x</sub>O<sub>2</sub> (x = 0.00 and x = 0.08) thick films were prepared from nanoparticles synthesized by the microwave-assisted hydrothermal route, aiming their application as a carbon monoxide sensing material to prevent deaths caused by this highly toxic gas. XRD analysis revealed that the nanopowders are free from secondary phases and crystallize in the fluorite cubic structure, which is confirmed by Raman spectroscopy. The Eu-doped ceria film presented much higher response (S) values than pure ceria, demonstrating the higher sensitivity of the doped system to carbon monoxide, especially at 400 °C. Electrical measurements under different atmospheres revealed a remarkably fast carbon monoxide response time for the Eu-doped film when compared with the pure sample, proving that the introduction of europium cations in the ceria lattice as dopants has a positive effect on the carbon monoxide sensing properties.

## 1. Introduction

Cerium dioxide (CeO<sub>2</sub>), also known as ceria, is a non-stoichiometric type-n semiconductor of great technological interest, which has been widely applied in multiple fields due to its remarkable properties [1–8]. Among the several methods to synthesize CeO<sub>2</sub> nanostructures that have been reported [9–20], the hydrothermal synthesis [10] stands out as a practical and useful technique to obtain high quality nanostructures of metal oxides, since it provides good control over homogeneity, particle size, chemical composition, phase formation and morphology of the resultant products [21]. The use of microwaves as the heating mechanism in the hydrothermal technique, opposed to the conventional method [21–26], has been described as a more environmentally friendly technique to synthesize ceramic nanostructures with lower temperature, lower power consumption and significant shorter time [8,22,27–29].

Ceria crystallizes in a fluorite structure with space group Fm3m and lattice parameter of 5.411 Å [30], where the cerium atoms are packed in a face centered cubic cell with oxygen atoms occupying tetrahedral sites. Alongside other rare-earth elements, cerium has unique properties due to an unfilled 4f orbital. Most applications are related to its Oxygen Storage Capacity (OSC), i.e. the ability to absorb or release oxygen, which is a result of cerium easy transition between oxidation states (Ce<sup>4+</sup>/Ce<sup>3+</sup>). During CeO<sub>2</sub> reduction, an oxygen vacancy is created together with the localization of an electron in a Ce 4f orbital [31]. This

process is explained by the Kröger-Vink notation as follows:



In order to maintain charge neutrality, a positive charged oxygen vacancy (Vo<sup>••</sup>) is created to compensate the negative effective charge generated after cerium reduction (2Ce<sub>Ce</sub><sup>'</sup>), resulting in a non-stoichiometric compound (CeO<sub>2-x</sub>). Therefore, an increase in oxygen vacancy concentration is expected when doping ceria with lower oxidation state cations. Accordingly, rare-earth elements (mostly trivalent cations, such as La<sup>3+</sup>, Gd<sup>3+</sup>, Eu<sup>3+/2+</sup> and Sm<sup>3+</sup>) have been extensively applied as ceria dopants due to their property similarity and the possibility of forming solid solutions, improving its activity, selectivity and thermal stability [32]. Also, the higher number of oxygen vacancies in the lattice promoted by rare-earth doping increases the conductivity and OSC, making it particularly interesting for gas sensing applications.

Carbon monoxide (CO) is a colorless, odorless and extremely toxic life-threatening gas known as the “Silent Killer”, due to its undetectable presence in the environment by humans. Therefore, a reliable and efficient CO sensor is needed to alert and protect potential victims from this threat. Gas sensor devices must not only have high sensitivity, stability, reversibility and selectivity, but also low cost and low energy consumption [33]. Fast response, reduced dimensions, portability and real time detection are other important parameters that must be considered [34]. Control over particle size and morphology plays a

\* Corresponding author.

E-mail address: [pedro.ortega@hotmail.com.br](mailto:pedro.ortega@hotmail.com.br) (P.P. Ortega).<https://doi.org/10.1016/j.apsusc.2018.09.142>

Received 12 June 2018; Accepted 17 September 2018

Available online 18 September 2018

0169-4332/ © 2018 Elsevier B.V. All rights reserved.

significant role when it comes to improving sensitivity. Particles with reduced size distribution lead to a higher surface-CO interaction and also allow the sensor to operate at lower temperatures and consume less energy [21,26]. Other important parameters that affect sensitivity are composition, surface modification, temperature, humidity and micro-structure [26].

The sensing mechanism in polycrystalline semiconductors is related to chemical reactions on the surface of the semiconductor when exposed to the target gas (e.g. carbon monoxide). The oxygen present in the atmosphere adsorbs on the surface and forms anionic oxygen ( $O^-$ ) by capturing electrons from the conduction band [35,36]. These electrons are then trapped by the oxygen species at the surface, creating an electron-depleted region and consequently decreasing the conductivity of the sensor. Subsequently, the exposure to the target gas promotes the oxidation of CO molecules by the adsorbed  $O^-$  to form carbon dioxide ( $CO_2$ ). The previously trapped electron then returns to the conduction band, which is followed by an increase in the conductivity [26,34,37]. Thus, the response of the sensor is measured by means of the electrical signal associated with variations in the conductivity during semiconductor-target gas interaction.

In previous work, we put great effort into characterizing and optimizing the preparation of pure and doped  $CeO_2$  thick films with nanostructures synthesized by the MAH method [27,29,38–40]. In this paper, we discuss the preparation and characterization of pure and europium-doped  $CeO_2$  thick films from the nanoparticles synthesized by the microwave-assisted hydrothermal method. The main goal is to evaluate their response as a CO sensing material and link this response to the microstructural modifications induced by europium doping.

## 2. Experimental procedure

### 2.1. Synthesis of the ceramic nanopowder

Nanopowders of  $Ce_{1-(3/4)x}Eu_xO_2$  ( $x = 0.00$  and  $x = 0.08$ ) were synthesized via microwave-assisted hydrothermal route. Ammonium cerium(IV) nitrate ( $(Ce(NH_4)_2(NO_3)_6)$ ) and europium(III) oxide ( $Eu_2O_3$ ) were used as precursors, both provided by Sigma-Aldrich with 99.0 and 99.9% purity, respectively. The cerium precursor was dissolved in aqueous media at 80 °C under constant magnetic stirring. In parallel, the europium oxide was dissolved under the same conditions, except for the addition of nitric acid ( $HNO_3$  65%, Synth) to assist with the dissolution process, and then added to the cerium solution. A  $2\text{ mol}\cdot\text{L}^{-1}$  potassium hydroxide solution (KOH 99.5%, Synth) was slowly added to the mixture at room temperature to adjust the pH to a value of 10. Subsequently, the mixture was transferred to a sealed Teflon autoclave and placed in a hydrothermal microwave oven (2.45 GHz, 800 W). The reactional system was heat treated at 100 °C for 8 min, with a heating rate of 10 °C/min, which are optimized parameters [38]. The resultant solution was transferred to centrifuge tubes, being then submitted to three cycles of washing with deionized water at 2000 rpm for 10 min each. Afterwards, the obtained  $Ce_{0.94}Eu_{0.08}O_2$  nanoparticles were dried at 100 °C for 48 h in an oven.

The obtained nanostructures were characterized by X-ray powder diffraction (XRD) using a Rigaku-DMAX/2500PC with  $Cu\text{-}K\alpha$  radiation ( $\lambda = 1.5406\text{ \AA}$ ) in the  $2\theta$  range from 20 to 80° with 0.2°/min. The Rietveld refinement was made with the software Topas 4.2. The Raman spectroscopy characterization was obtained by a LabRAM iHR550 Horiba Jobin Yvon spectrometer with a 514 nm wavelength laser as excitation source and spectral resolution of  $1\text{ cm}^{-1}$ , with 40 scans in the range of 100–1500  $\text{cm}^{-1}$ , coupled to a CCD detector. The procedure was made with an Argon-ion laser, whose wavelength is 514.5 nm and with a power of 8 mW. Ultraviolet–visible (UV–vis) spectroscopy for the optical absorbance spectra was taken using a Cary 5G (Varian, USA) spectrophotometer in diffuse reflection mode and the band gap energy was obtained by means of the Tauc's method, which is based on the relationship between diffuse reflectance and band gap given by the

following equation:

$$(h\nu\alpha)^{1/n} = A(h\nu - E_g) \quad (2)$$

where  $\alpha$  is the absorption coefficient,  $h\nu$  is the photon energy,  $A$  is a constant and  $E_g$  is the band gap. The  $n$  value depends on the nature of the electronic transitions: direct allowed ( $n = 1/2$ ), direct forbidden ( $n = 3/2$ ), indirect allowed ( $n = 2$ ) and indirect forbidden ( $n = 3$ ). Therefore, considering direct allowed transition, the equation is:

$$(h\nu\alpha)^2 = A(h\nu - E_g) \quad (3)$$

The plot of  $(h\nu\alpha)^2$  in function of  $h\nu$  is known as the Tauc plot. The extrapolation of the linear portions of the curves until it intersects the axis where absorption is zero gives the band gap energy. The high resolution transmission electron microscopy (HRTEM) images were taken at room temperature by dispersing the nanoparticles obtained by the MAH method in ethanol and, after drying, adding them to a 300 mesh copper grade, followed by ultrasonic vibration for 5 min. The microscope used was a FEI TECNAI F20.

### 2.2. Preparation of the films

A paste, based on a mixture of the nanopowder obtained from the MAH synthesis and an organic binder (glycerol), was used to prepare thick porous films by the screen-printing technique onto 96% dense insulating alumina substrates, on which a 25 nm titanium (Ti) adhesion layer and a 200 nm platinum layer had been deposited by RF-Sputtering. The interdigitated platinum (Pt) electrodes were delineated by a home-built micromachining laser. The substrate dimensions are  $20 \times 10\text{ mm}$  (length  $\times$  width) and the Pt electrodes have a resistance of  $10\ \Omega$ . The powder/binder ratio used was 1.6 g/ml. After deposition, the films were heat treated in dry air atmosphere with 1 °C/min steps up to 380 °C and maintained in this temperature for 2 h, in order to evaporate the binder. An illustration of the deposited film is shown in Fig. 1.

The surface morphology of the film was observed using a high-resolution field-emission gun scanning electron microscope (FEG-SEM) Supra 35-VP (Carl Zeiss, Germany). The film thickness was measured with a Surtronic 3+ (Taylor Hobson) profilometer with a diamond stylus (radius: 1  $\mu\text{m}$ ) and the cross section was analyzed using SEM microscopy. The electrical resistance measurements were carried out in function of time (at 400 °C) and temperature, in vacuum, dry air and CO atmospheres at a constant pressure of 100 mmHg. The electrical measurements were made in a optoelectronic device (Patent INPI Argentina 201501039539/INPI Brazil 10 2016 028383 3 [41,42]) consisting of a closed chamber in which three cycles of heating in vacuum up to 380 °C were made before measuring the resistance values, assuring the volatilization of any humidity. The measurements were made when the samples got to a steady state and no changes in resistance over time were observed, with an applied magnitude of excitation current of 1 mA, obtained using the two-wire technique with a DC-type measurement. An Agilent 3440A multimeter was used for the electrical resistance measurements.

## 3. Results and discussion

### 3.1. Characterization of the nanoparticles

In order to confirm the formation of a Ce-Eu solid solution, X-Ray Diffraction (XRD) analysis of the crystalline phases was carried out (Fig. 2). The XRD patterns for both pure and europium doped ceria show all the characteristic peaks of the  $CeO_2$  fluorite structure (JCPDS 34-0390) [27] and no peaks of any other phase were detected. The absence of diffraction peaks belonging to  $Eu_2O_3$  phase indicates the isomorphic substitution of cerium by europium cations in the lattice and/or that it might be present in a highly dispersed state [32]. A small shift of diffraction peaks towards lower angles can be observed in the

Download English Version:

<https://daneshyari.com/en/article/10155089>

Download Persian Version:

<https://daneshyari.com/article/10155089>

[Daneshyari.com](https://daneshyari.com)